Plane oxygen vibrations and their temperature dependence in $HgBa_2Ca_2Cu_3O_{8+\delta}$ single crystals

Xingjiang Zhou* and M. Cardona
Max-Planck-Institut für Festkörperforschung, Heisenbergstrasse 1, D-70569 Stuttgart, Germany

D. Colson and V. Viallet
CEA, Saclay, Service de Physique de l'Etat Condensé, DRECAM/SPEC, 91191 Gif sur Yvette Cedex, France
(Received 20 December 1996)

A polarized Raman-scattering investigation of $HgBa_2Ca_2Cu_3O_{8+\delta}$ single crystals has been performed. The following Raman-active modes associated with oxygen vibrations in the CuO_2 planes have been clearly identified: the B_{1g} mode at 245 cm^{-1}, corresponding to the out-of-phase vibration of the plane oxygens, and the A_{1g} mode at 265 cm^{-1}, corresponding to their in-phase vibration. Another defect-induced A_{1g} mode was also detected at 400 cm^{-1}. Measurements of the temperature dependence of these Raman features demonstrate that the A_{1g} 265- and 400-cm^{-1} modes show abrupt changes in frequency and linewidth across T_c, accompanied by an appreciable intensity enhancement in the superconducting state. However, similar ''anomalies'' were not observed for the 245-cm^{-1} phonon of B_{1g} symmetry. [S0163-1829(97)00518-3]

I. INTRODUCTION

In superconductors, the opening of the superconducting gap leads to a redistribution of electronic states near the Fermi surface which can in turn result in changes of phonon frequency, linewidth, as well as intensity of some phonons across the superconducting transition temperature (T_c). In $YBa_2Cu_3O_{7-\delta}$ (Y-123), e.g., Raman scattering revealed a considerable frequency softening and linewidth broadening (or sharpening, depending on exact stoichiometry) of the B_{1g}-like mode at 340 cm^{-1}, associated with the out-of-phase c-axis vibrations of the plane oxygens, below T_c.[1,2] Inelastic neutron-scattering measurements further demonstrated that the softening and linewidth broadening of phonons of the same branch show strong anisotropy for different directions of the wave vectors $\mathbf{q}$.[3] On the other hand, the A_{1g}-like mode at 440 cm^{-1}, associated with the in-phase c-axis vibrations of the plane oxygens, hardens below T_c.[4] These superconductivity-induced self-energy effects clearly signal a coupling between these phonons and the electronic states which can be used to probe the magnitude and even the symmetry of the superconducting order parameter.[1,3]

The $HgBa_2Ca_2Cu_3O_{8+\delta}$ superconductor (referred to as Hg-1223 hereafter) has attracted much interest because of its record high critical temperature (T_c=136 K) at ambient pressure[5] and its remarkable additional enhancement under high pressures.[6] Raman scattering, with other techniques,[7,8] can act as a tool to probe the low-lying elementary excitations associated with the CuO_2 planes, which are essential to investigate the mechanism of high-T_c superconductivity.[9] So far a number of Raman-scattering measurements have been performed on Hg-1223.[10–16] Most of these are micro-Raman measurements and were performed for microcrystalline samples in zz polarization for which the phonon features are strong and mainly associated with vibrations of the apical and excess oxygens. However, only a few phonon features could be observed in a-b plane spectra and the plane oxygen vibrations were not explicitly identified, even in a Hg-1223 single crystal.[14,16]

In this paper, we report an analysis of the complete polarized Raman spectra of a $HgBa_2Ca_2Cu_3O_{8+\delta}$ single crystal. In addition to reexamining the previous Raman results in zz and zx polarizations, we have clearly observed vibrational features from the a-b plane spectra which allow unambiguous identification of vibrations of the oxygens in the CuO_2 planes. We have investigated the temperature dependence of these vibrational features and find that the A_{1g} vibrations show abrupt changes at T_c when the sample enters from the normal to the superconducting state. However, such superconductivity-induced effects are not observed for the B_{1g} mode.

II. EXPERIMENTAL

The Hg-1223 single crystal under measurement was grown by a single-step synthesis method under normal pressure.[17] It has a tetragonal structure with the $P4/mmm$ space group: the equivalent a-b axes are along the Cu-O direction, while the c axis is perpendicular to the CuO_2 plane.[18] This parallelepiped-shaped, as-grown sample has a size of $\sim 0.6\times 0.6\times 0.2$ mm^3 with a smooth (001) surface and its c axis is along the thinnest dimension. Within the square (001) plane the a-b axes lie along the diagonal directions. Magnetization measurements show that it has a T_c=130 K, as defined by the onset of the diamagnetism, with a transition width of $\sim$10 K.

Polarized Raman spectra were measured with a Dilor XY triple spectrometer equipped with a CCD detector in a near-backscattering geometry. The samples were kept in a vacuum in a cryostat and measured at both room and low temperatures. We measured the Raman spectra on the Hg-1223 single crystal with different laser lines generated by a mixed gas (Ar^+ and Kr^+) laser and found that the red line (647.1-nm wavelength) is more favorable for identifying weak phonon features.

III. RESULTS AND DISCUSSION

We have measured the Raman spectra of Hg-1223 single crystal in various polarizations. For convenience, the polar-

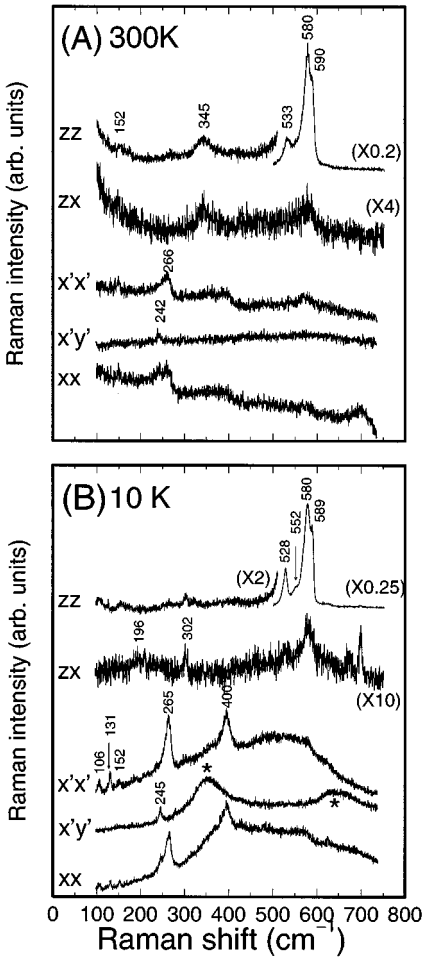

FIG. 1. Polarized Raman spectra of a Hg-1223 single crystal measured with 647.1-nm laser excitation at room temperature (a) and at 10 K (b), respectively. (b) the broad peaks in $x'y'$ polarization at 370 and 665 cm^{-1} (marked by *) are due to redistribution of the electronic continuum in the superconducting state.

ization geometry is denoted by ij, with i and j representing the polarization of the incident and scattered light, respectively. The coordinates x, y, and z correspond to directions along the two equivalent a axes and the c axis, respectively, while x' and y' represent the two diagonal in-plane directions.

Figure 1 shows a complete set of polarized Raman spectra of Hg-1223 measured with the 647.1-nm laser line at room temperature [Fig. 1(a)] and at 10 K [Fig. 1(b)]. Strong peaks show up in the zz polarization while the phonon features are considerably weaker when the incident and scattered light are polarized in the a-b plane. Nevertheless, such weak features are discernible in the spectra measured at room temperature [Fig. 1(a)] and become more prominent at low temperatures [Fig. 1(b)]. In addition, when comparing the spectra measured at room temperature and at 10 K, we observe an obvious spectral redistribution when the sample enters the superconducting state which will be discussed elsewhere.[19]

The Raman spectra in zz and zx polarizations were measured at several different positions on the edge of the sample. The purpose was to sort out possible weak features from artifacts caused by minor amount of impurity phases which may adhere to the sample. In zz polarization prominent peaks at 589, 580, 552, and 528 cm^{-1} (10 K) can be observed. These features, and a few others in the 450−600 cm^{-1} range, have been extensively investigated in polycrystalline samples and assigned to vibrations of the apical oxygens and the excess oxygens: they depend strongly on the excess oxygen content δ.[15,16] We noticed that the spectra in this range showed a slight difference when measuring at different positions, which probably reflects a slight inhomogeneity of the excess oxygen distribution on the edge of the sample. Comparing these spectra with that measured on another optimally doped Hg-1223 single crystal with $T_c=136$ K also allows us to determine that this Hg-1223 single crystal with $T_c=130$ K is slightly underdoped. The features in this range show little temperature dependence except for the 528-cm^{-1} peak which softens by nearly 5 cm^{-1} when the sample is cooled from room temperature to 10 K.

Besides the strong peaks described above, some additional weak peaks are observed in zz polarization at 700, 676, 623, 400, 345, 302, 264, 152, 131, and 106 cm^{-1} summerized for different positions (not all of them are visible in Fig. 1). Some of them, such as those at 400, 264, 152, 131, and 106 cm^{-1}, are reproducible at different positions. Therefore, we believe that they are intrinsic to the Hg-1223 structure and have A_{1g} symmetry. The appearance of the remaining peaks depends on the position of the laser spot and their presence in zx polarization indicates that they do not obey strict selection rules; they can thus be attributed to some impurity phases. The three lowest frequency modes at 106, 131, and 152 cm^{-1}, of A_{1g} symmetry, apparently correspond to (possibly mixed) vibrations of the metal ions since Ca, Ba, and Cu each contributes one Raman-active A_{1g} mode in Hg-1223.[16]

In zx polarization geometry the measured spectra are extremely weak. Only phonons with E_g symmetry are allowed in this polarization and six E_g modes are predicted by group theory for Hg-1223.[14,16] The peaks observed in zx polarization summarized for different positions have the following frequencies: 700, 676, 580, 530, 345, 302, 260, 245, 195, 174, and 118 cm^{-1}. Among them, the 700, 676, 345, and 302 cm^{-1} peaks have been earlier attributed to impurity phases. The broad 580 and 530 cm^{-1} peaks are likely to be due to leakage of the strong features in zz polarization. The 260 and 245 cm^{-1} peaks are also likely to arise from polarization leakage since they appear strongly in xx and $x'x'$ polarization. The remaining 195, 174, and 118 cm^{-1} peaks are not always reproducible at different laser spot positions, although some of them, like the 195 cm^{-1} peak, may correspond to the E_g modes, as suggested previously.[16] However, we did not observe the series of peaks reported earlier for the zx polarization.[14]

Of particular interest is the observation of Raman-active modes when the electric fields of the incident and scattered light are within the a-b plane. These modes have not been reported before.[14] Beside the low-frequency peaks corresponding to metal-ion vibrations, three additional peaks can be seen in the in-plane spectra at 245, 265, and 400 cm^{-1} (Fig. 1). In $x'y'$ polarization, only a B_{1g} mode is allowed: the 245 cm^{-1} peak [Fig. 1(b)], absent in $x'x'$ polarization

and present in xx polarization, has definitely B_{1g} symmetry. With three consecutive CuO_2 planes within one unit cell, this mode corresponds to the out-of-phase vibration of the oxygens within the highest and lowest CuO_2 planes, while the oxygens in the intermediate plane remain stationary. For the B_{1g} mode the upper and lower CuO_2 plane oxygens vibrate in opposite directions. The frequency of this mode is close to that of the B_{1g} mode in the isomorphic Tl-1223 compound which has been observed at 238 cm^{-1} (Ref. 20) and calculated to lie at 260 cm^{-1}.[21] Compared with the frequency of the B_{1g} mode in bilayer compounds such as Tl-1212 (measured at 278 cm^{-1}),[22] the slightly lower frequencies for these three plane compounds are likely to arise from the larger distance between the vibrating CuO_2 planes.

The other two peaks observed in xx and $x'x'$ polarizations at 265 and 400 cm^{-1}clearly have A_{1g} symmetry. Given that only two oxygen-related A_{1g} modes are predicted for defectless Hg-1223,[16] and one of them, the mode associated with the apical oxygen, has a high frequency around 590 cm^{-1}, as expected for oxygen bond-stretching vibrations, one of these lower frequency A_{1g} modes may correspond to a plane oxygen bond-bending mode. In Tl-1223, this A_{1g} mode has a measured frequency of 260 cm^{-1} (Ref. 20) and a calculated frequency of 293 cm^{-1}.[21] Hence the A_{1g} peak seen at 265 cm^{-1} in Hg-1223 should represent the same type of oxygen vibration, corresponding to in-phase vibration within the highest and lowest CuO_2 planes, while the middle plane remains stationary. The 400-cm^{-1} mode has to be a defect-induced mode which can be assigned as a mixed vibration involving excess oxygen and the oxygens in the CuO_2 planes.[16]

The plausible mode identification of the plane oxygen vibrations in Hg-1223 makes it desirable to further examine their temperature dependence, particularly in the vicinity of T_c. Typical spectra of the A_{1g} 265- and 400-cm^{-1} modes measured in $x'x'$ polarization between 10 and 300 K are shown in Fig. 2(a) and Fig. 4(a) while the B_{1g} 245-cm^{-1} mode measured in $x'y'$ polarization is shown in Fig. 3(a). The 265- and 400-cm^{-1} peaks display clearly asymmetric line shapes which suggest interaction between these discrete (phonon) states and a broad (electronic) continuum.[9] We have fitted the measured spectra with a standard Fano function:

$$I(\omega)=C\frac{(\epsilon+q)^2}{1+\epsilon^2}+\ \text{background}, \qquad (1)$$

in which $\epsilon=(\omega-\omega_p)/\Gamma$, ω_p being the phonon frequency, q is the Fano line-shape parameter, Γ is a linewidth contribution, and C is a scaling factor. The fitted values of these parameters and the integrated intensities ($=\pi C\Gamma q^2$) of the 265- and 400-cm^{-1} peaks are plotted in Fig. 2(b) and 4(b). The B_{1g} 245-cm^{-1} peak is nearly symmetric and was therefore fitted with a simple Lorentzian: the fitting parameters are shown in Fig. 3(b).

In Fig. 2(b) we include two data sets deduced separately from the spectra measured with the 647.1- and 568.2-nm laser lines. Although there is considerable scattering in the experimental points because of the weak nature of the 265-cm^{-1} peak, especially at temperatures above 200 K, an overall frequency softening, a linewidth narrowing, an increase of $-q$, and an enhancement of the integrated intensity can be clearly seen around T_c when going from the normal to the superconducting state. The frequency shifts downward by 3–4 cm^{-1} in the temperature range between 80 and 130 K, corresponding to a relative softening $\Delta\omega/\omega=1.1$ to 1.5%. The accompanying linewidth narrowing in the same temperature range is nearly 6 cm^{-1}, corresponding to $\Delta(2\Gamma)/\omega=2.3\%$. The absolute linewidth parameter $(-q)$ increases with decreasing temperature from nearly 2.5 above T_c to 6 at 10 K. The integrated intensity keeps increasing from T_c down to 10 K by about a factor of 3.

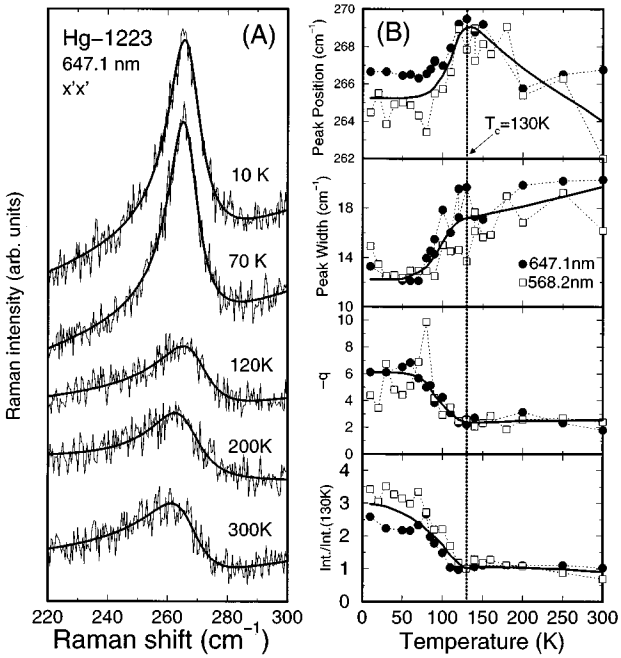

FIG. 2. Representative Raman spectra of the 265 cm^{-1} A_{1g} mode measured in $x'x'$ polarization with the 647.1-nm laser line at different temperatures and the corresponding fitted Fano profiles (a). The fitted frequency, linewidth (2Γ), line-shape parameter (q), and the integrated intensity (normalized to the intensity at 130 K) are plotted in (b) as solid circles (●). Also included are parameters as empty squares (□) obtained by fitting the spectra measured with 568.2-nm laser excitation. The solid lines are guides to the eye.

The temperature dependence of the B_{1g} phonon observed at 245 cm^{-1} is shown in Fig. 3. This peak was too weak when measured with the 568.2-nm laser line to extract reliable parameters and therefore only the data measured with 647.1-nm laser excitation are presented. In contrast to the A_{1g} 265-cm^{-1} peak, the corresponding phonon frequency shows a monotonic increase from 242 to 246 cm^{-1} from room temperature to 10 K. In the same temperature range its linewidth (full width at half maximum, FWHM) displays a considerable narrowing from 14 to 4 cm^{-1} with decreasing temperature. This corresponds to the standard behavior in many solids. It can be described by a temperature-dependent anharmonic decay of the Raman-active phonon with frequency ω and zero wave vector $\mathbf{q}$ into two phonons with opposite wave vectors and frequencies close to $\omega/2$. The corresponding temperature dependence of the linewidth is given by[23]

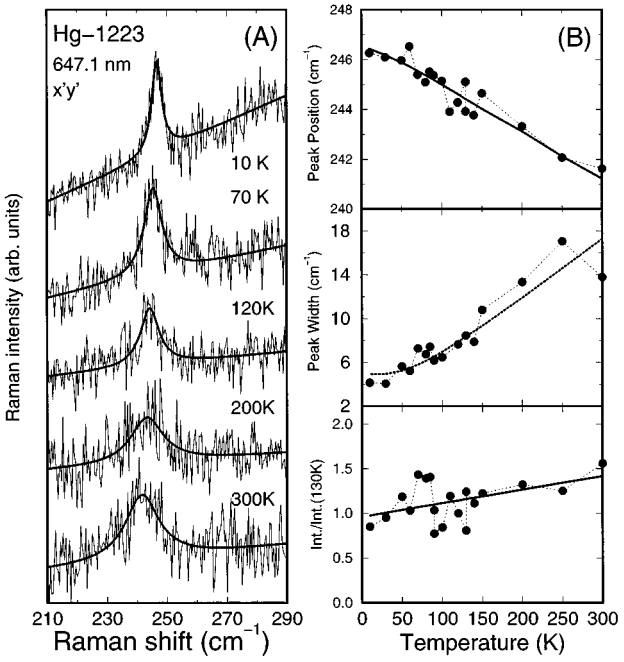

FIG. 3. Spectral variation of the 245-cm^{-1} B_{1g} phonon measured in $x'y'$ polarization with 647.1-nm laser excitation at different temperatures and the corresponding Lorentzian fitting curves (a). The fitted frequencies, linewidths (FWHM) and normalized integrated intensities are displayed in (b). The solid lines are guides to the eye. The dotted line in the linewidth panel represents a fit with $\Gamma(T)=\Gamma(0)[1+2/e^{\hbar\omega/2k_BT}-1]$, taking $\omega=245$ cm^{-1}, which yields $\Gamma(0)=4.9$ cm^{-1}.

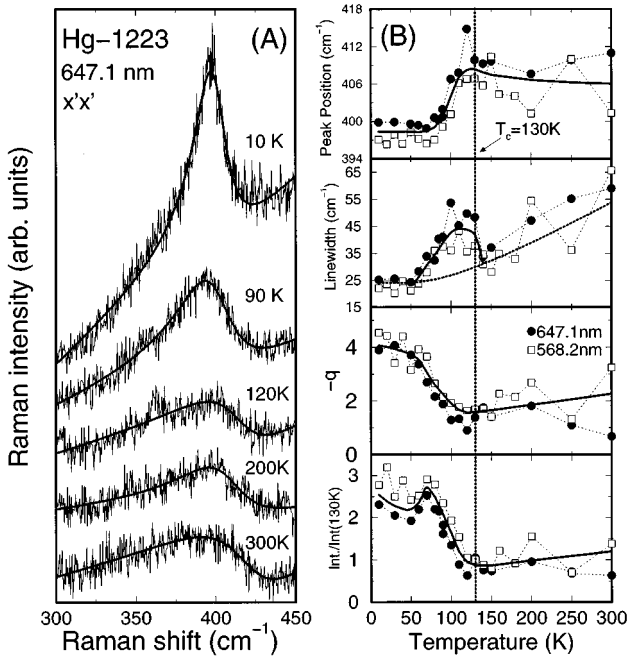

FIG. 4. Representative Raman spectra covering the 400-cm^{-1} A_{1g} mode measured in $x'x'$ polarization with the 647.1-nm laser line at different temperatures and the corresponding fits with Fano profiles (a). The fitted frequencies, linewidths (2Γ), line-shape parameters (q), and the normalized integrated intensities are represented in (b) by solid circles (●). Also included as empty squares (□) is another data set which corresponds to the spectra measured with 568.2-nm laser excitation. The solid lines are guides to the eye while the dotted line in the linewidth panel represents the fit with $\Gamma(T)=\Gamma(0)[1+2/e^{\hbar\omega/2k_BT}-1]$, taking $\omega=400$ cm^{-1}, which yields $\Gamma(0)=24$ cm^{-1}.

$$\Gamma(T)=\Gamma(0)\left(1+\frac{2}{e^{\hbar\omega/2k_BT}-1}\right). \tag{2}$$

The dotted line in Fig. 3(b) represents the fit with Eq. (2) for $\Gamma(0)=4.9$ cm^{-1} taking $\omega=245$ cm^{-1}. This fit is in rather good agreement with the measured data. The integrated intensity of the 245 cm^{-1} peak also remains nearly constant between room temperature and T_c. The peak position, linewidth, and intensity vary smoothly around T_c. No anomalies of the type observed for the 265 cm^{-1} mode can be identified.

The 400-cm^{-1} A_{1g} mode, however, shows again abrupt changes across T_c (Fig. 4). Above T_c, this peak is very broad and weak, far broader than the other two phonons, a fact which may further substantiate its defect-induced nature. Upon entering the superconducting state, the peak decreases its frequency by 10 cm^{-1} from T_c down to 70 K ($\Delta\omega/\omega=2.5\%$). It also shows a considerable sharpening ($\sim$40 cm^{-1}) from room temperature to 10 K. The data above T_c and well below T_c can also be fitted by Eq. (2) with $\Gamma(0)=24$ cm^{-1} (dotted line in Fig. 4). By subtracting this contribution of anharmonic decay into two phonons, we are left with an increase of 16 cm^{-1} below T_c [$\Delta(2\Gamma)/\omega=4.0\%$] which can be attributed to superconductivity. In the superconducting state the absolute Fano line-shape parameter shows an increase from 1.6 to 4.0, while the integrated intensity increases by a factor of 2.5. Note that below T_c, a peak in the integrated intensity appears near 70 K.

It is interesting to contrast the plane oxygen vibrations in Hg-1223 with those in Y-123.[9] In the latter, the B_{1g}-like mode at 340 cm^{-1} shows an asymmetric line shape, which has been analyzed in terms of a charge-transfer fluctuation between the in-plane oxygens and the apical oxygen[24] or between the in-plane oxygens themselves,[25] whereas the A_{1g}-like mode at 440 cm^{-1} is nearly symmetric. In Hg-1223, however, the B_{1g} mode is nearly symmetric whereas the A_{1g} modes at 265 and 400 cm^{-1} show an asymmetric line shape. Moreover, the B_{1g}-like mode in Y-123 shows an anomalous frequency softening, below T_c, accompanied by strong changes in linewidth and an intensity enhancement. In Hg-1223, however, such changes appear for the two A_{1g} modes, while none can be detected for the B_{1g} mode.

The anomalous self-energy effects at T_c are known to be directly proportional to the electron-phonon coupling constant.[26] The coupling between the phonons and the in-plane electrons has been proposed to be related to the buckling of the CuO_2 planes: the coupling constant is very small for flat CuO_2 planes.[4] The lack of T_c anomalies observed for the B_{1g} 245-cm^{-1} phonon seems to support this conjecture since in Hg-1223 the CuO_2 planes are nearly flat.[27] However, the sizable self-energy effects observed for the A_{1g} 265-cm^{-1} phonon are hard to explain on this basis. One alternative mechanism may be the electron-phonon coupling resulting from crystal-field effects due to the asymmetric en-

vironment surrounding the CuO_2 planes, but for phonons with A_{1g} symmetry, the predicted coupling remains vanishingly small.[25] Therefore, the microscopic origin of the electron-phonon coupling for these A_{1g} phonons remains unclear.

The abrupt changes in the frequency and linewidth of the 245- and 400-cm^{-1} phonons across T_c can be attributed to changes in the real and imaginary parts of the phonon self-energies, $\Delta\Sigma=\Delta\omega-i\Delta\gamma$ induced by the superconducting transition.[26,28,29] The real part of the self-energy change ($\Delta\omega$) renormalizes the peak position, while the change of the imaginary part ($-\Delta\gamma$) should effect the phonon linewidth. Within the framework of strong-coupling Eliasberg theory, a characteristic dependence of the self-energy change on the ratio of the phonon frequency ω (at T_c) to the gap 2Δ has been predicted.[26,29] Qualitatively speaking, phonons below the gap should exhibit some softening which decreases with increasing separation from the gap 2Δ. Phonons above the gap, on the other hand, should harden slightly in the clean case although this effect may turn into a small softening if impurity scattering is taken into account.[26] For a given phonon the self-energy effects are expected to be strongest when the phonon energy is close to resonance with the gap.

We have seen that between T_c and 10 K, the peaks at 245, 265, and 400 cm^{-1} show superconductivity-induced relative frequency softenings of 0, 1.1, and 2.5%, respectively. The more pronounced effects observed for the A_{1g} 400-cm^{-1} mode suggests that its energy is close to 2Δ. We have observed multicomponent gap features in the electronic Raman scattering of B_{1g} symmetry, with peaks at 370 and 665 cm^{-1} (Ref. 19) [see also Fig. 1(b)]. The 370-cm^{-1} peak appears below 80 K, while the 665 cm^{-1} peak becomes prominent just below $T_c=130$ K. The A_{1g} spectrum [see $x'x'$ configuration in Fig. 1(b)] exhibits a broad electronic band with a maximum slightly above 400 cm^{-1}. The latter would explain the self-energy effects observed for the 400-cm^{-1} vibrational structure, a fact which suggests that $2\Delta \geqslant 400$ cm^{-1}. This would lead to a value of $2\Delta/T_c \simeq 4.6$, higher than the standard BCS value but in the lower range of gaps observed for other high-T_c superconductors.

The large broadening of the 400-cm^{-1} vibrational structure immediately below T_c [$\Delta(2\Gamma)/\omega \sim 4.0\%$, see Fig. 4] also implies that the superconducting gap 2Δ is slightly above 400 cm^{-1}. Below T_c 2Δ becomes equal to 400 cm^{-1} and provides an additional decay channel leading to an increase of phonon linewidth.[26,29] At the lowest temperatures the phonon is well in the gap, a fact which results in a sharpening as decay channels are being removed. This mechanism must be modified in order to account for the sharpening of the 265 cm^{-1} structure which we have assumed to correspond to a phonon with a well-defined **q** vector. In this case no self-energy broadening would be present in the normal state and, correspondingly, no sharpening should occur. However, sharpenings have also been observed for some low-frequency phonons in Y-123 (Refs. 2 and 30) and $YBa_2Cu_4O_8$.[31] In order to account for these sharpenings we must assume considerable relaxation of the **k** conservation so as to have Landau damping at the frequencies under consideration, even for $\mathbf{k} \simeq 0$.

We note in Figs. 2 and 4 that, for the 265- and 400-cm^{-1} modes, anomalies in the phonon self-energies at T_c are also accompanied by an increase (a factor of 3) in the integrated intensity below T_c. A careful inspection may further reveal two intensity anomalies at 130 and 70–80 K, which correspond to the appearance of the two superconducting gaps identified in the electronic Raman scattering.[19] Therefore, like in the case of the phonon self-energy effects, the scattering intensity enhancement below T_c appears to originate also from large electron-phonon interaction around the Fermi surface. Since vibrational Raman scattering is mediated by electronic excitations and the scattering intensity determined by electron-phonon interaction and electron-radiation interaction for different electron bands summed over all possible intermediate states (channels), some of these channels may approach resonant Raman scattering, thus increasing the scattering efficiency. Therefore, the superconductivity-induced intensity enhancement may reflect resonant Raman effects resulting from the shift and other modifications of the excitations around the Fermi surface produced by the opening of the gap.[31] Such effects are expected to be particularly strong if the vibrational states being considered interact strongly with the electrons around the Fermi surface, as is the case for the 265- and 400-cm^{-1} modes.

IV. CONCLUSIONS

We have carried out Raman-scattering measurements on $HgBa_2Ca_2Cu_3O_{8+\delta}$ single crystals at different temperatures and for all polarization configurations. The phonon modes associated with the plane oxygen vibrations have been explicitly identified in the *a-b* plane spectra: the only possible B_{1g} mode, observed at 245 cm^{-1}, is associated with the out-of-phase vibration of the oxygens in the CuO_2 planes, while the A_{1g} mode at 265 cm^{-1} corresponds to the in-phase vibration. An additional defect-induced vibrational mode of A_{1g} symmetry is also observed at 400 cm^{-1}. Measurements of the temperature dependence of these modes indicate that the two A_{1g} vibrations show clearly frequency softening, linewidth narrowing (broadening for the 400-cm^{-1} mode), and intensity enhancement when the sample enters from the normal into the superconducting state. Such abrupt changes are not observed for the B_{1g} mode at 245 cm^{-1}, a fact which seems to be related to the lack of buckling in the CuO_2 planes.

ACKNOWLEDGMENTS

We thank H. Hirt and M. Siemers for expert technical help and T. Strach for a critical reading of the manuscript. X.J.Z. acknowledges the Alexander von Humboldt Foundation for financial support and hospitality.

*On leave from National Lab for Superconductivity, Institute of Physics, Chinese Academy of Sciences, Beijing 100080, China.
[1] B. Friedl, C. Thomsen, and M. Cardona, Phys. Rev. Lett. **65**, 915 (1990).
[2] E. Altendorf, X. K. Chen, J. C. Irwin, R. Liang, and W. N. Hardy, Phys. Rev. B **47**, 8140 (1993).
[3] D. Reznik, B. Keimer, F. Dogan, and I. A. Aksay, Phys. Rev. Lett. **75**, 2396 (1995).
[4] C. Thomson, M. Cardona, B. Friedl, I. I. Mazin, O. Jepsen, O. K. Anderson, and M. Methfessel, Solid State Commun. **75**, 219 (1990).
[5] A. Schilling, M. Cantoni, J. D. Guo, and H. R. Ott, Nature (London) **363**, 56 (1993).
[6] L. Gao, Y. Y. Xue, F. Chen, Q. Xiong, R. L. Meng, D. Ramirez, C. W. Chu, J. H. Eggert, and H. K. Mao, Phys. Rev. B **50**, 4260 (1994).
[7] M.-H. Julien, P. Carretta, M. Horvatić, C. Berthier, Y, Berthier, P. Ségransan, A. Carrington, and D. Colson, Phys. Rev. Lett. **76**, 4238 (1996).
[8] K. Magishi, Y. Kitaoka, G.-q. Zheng, K. Asayama, K. Tokiwa, A. Iyo, and H. Ihara, Phys. Rev. B **53**, R8906 (1996).
[9] C. Thomson, in *Light Scattering in Solids*, edited by M. Cardona and G. Güntherodt (Springer, Berlin, 1991), Vol. 6 .
[10] Y. T. Ren, H. Chang, Q. Xiong, Y. Q. Wang, Y. Y. Sun, R. L. Meng, Y. Y. Xue, and C. W. Chu, Physica C **217**, 273 (1993).
[11] H. Chang, Z. H. He, R. L. Meng, Y. Y. Yue, and C. W. Chu, Physica C **251**, 126 (1995).
[12] I. S. Yang, H. G. Lee, H. S. Shin, J. H. Park, S. I. Lee, and S. Lee, Physica C **222**, 386 (1994).
[13] I. S. Yang, H. G. Lee, N. H. Hur, and J. J. Yu, Phys. Rev. B **52**, 15 078 (1995).
[14] A. Sacuto, A. Lebon, D. Colson, A. Bertinotti, J.-F. Marucco, and V. Viallet, Physica C **259**, 209 (1996).
[15] X. J. Zhou, M. Cardona, C. W. Chu, Q. M. Lin, S. M. Loureiro, and M. Marezio, Phys. Rev. B **54**, 6137 (1996).
[16] X. J. Zhou, M. Cardona, C. W. Chu, Q. M. Lin, S. M. Loureiro, and M. Marezio, Physica C, **270**, 193 (1996).
[17] D. Colson, A. Bertinotti, J. Hammann, J. F. Marucco, and A. Pinatel, Physica C **233**, 231 (1994).
[18] A. Bertinotti, D. Colson J. Hammann, J. F. Marucco, A. Pinatel, and V. Viallet, Physica C **250**, 213 (1995).
[19] X. J. Zhou, M. Cardona, D. Colson, and V. Viallet, Phys. Status Solidi B **199**, R7 (1997).
[20] K. F. McCarty, B. Morosin, D. S. Ginley, and D. R. Boehme, Physica C **157**, 135 (1989).
[21] A. D. Kulkarni, F. W. de Wette, J. Prade, U. Schröder, and W. Kress, Phys. Rev. B **41**, 6409 (1990).
[22] K. F. McCarty, D. S. Ginley, D. R. Boehme, R. J. Baughman, E. L. Venturini, and B. Morosin, Physica C **156**, 119 (1988).
[23] J. Menéndez and M. Cardona, Phys. Rev. B **29**, 2051 (1984).
[24] H. Monien and A. Zawadowski, Phys. Rev. Lett. **63**, 911 (1989).
[25] T. P. Devereaux, A. Virosztek, and A. Zawadowski, Phys. Rev. B **51**, 505 (1995).
[26] R. Zeyher and G. Zwicknagl, Z. Phys. B **78**, 175 (1990).
[27] J. L. Wagner, B. A. Hunter, D. G. Hinks, and J. D. Jorgensen, Phys. Rev. B **51**, 15 407 (1995).
[28] S. M. Shapiro, G. Shirane, and J. D. Axe, Phys. Rev. B **12**, 4899 (1975).
[29] E. J. Nicol, C. Jiang, and J. P. Carbotte, Phys. Rev. B **47**, 8131 (1993).
[30] B. Friedl, C. Thomson, H.-U. Habermeier, and M. Cardona, Solid State Commun. **81**, 989 (1992).
[31] E. T. Heyen, M. Cardona, J. Karpinski, E. Kaldis, and S. Rusiecki, Phys. Rev. B **43**, 12 958 (1991).